Pergamon

Bioorganic & Medicinal Chemistry Letters, Vol. 5, No. 4, pp. 343-348, 1995
Copyright © 1995 Elsevier Science Ltd
Printed in Great Britain. All rights reserved
0960-894X/95 $9.50+0.00

0960-894X(95)00032-1

HYDROXAMATE INHIBITORS OF THE MATRIX METALLO-PROTEINASES (MMPs) CONTAINING NOVEL P_1' HETEROATOM BASED MODIFICATIONS

Bruce E. Tomczuk*, Madhusudhan R. Gowravaram, Jeffrey S. Johnson, Daniel Delecki, Ewell R. Cook, Arup K. Ghose, Alan M. Mathiowetz, John C. Spurlino, Byron Rubin, Douglas L. Smith, Tricia Pulvino and Robert C. Wahl

Sterling Winthrop Pharmaceuticals Research Division, 1250 S. Collegeville Road, P.O. Box 5000, Collegeville, PA 19426-0900

Abstract: Structure-based drug design (SBDD) and traditional SAR have guided the development of potent and selective hydroxamate inhibitors which contain heteroatom-based modifications of the P_1' group. These inhibitors may help delineate the *in vivo* roles of specific MMPs in normal and disease states.

Enzymes of the matrix metallo-proteinase (MMP) family, such as human fibroblast collagenase (HFC) and human fibroblast stromelysin (HFS), are hypothesized to be major degradative factors of the structural components of articular cartilage.[1] Increased levels of these enzymes have been observed in the cartilage and synovium of patients with rheumatoid and osteoarthritis and correlate to the severity of the disease.[2] Thus, inhibitors of these enzymes should provide disease-modifying treatment for these diseases. However, these enzymes may also be involved in the normal maintenance or repair of these tissues.[3] Only potent, selective, and bioavailable inhibitors will delineate the roles of these enzymes in normal and disease states.

There are several known classes of inhibitors of MMPs, such as hydroxamates, thiols, phosphorus-types (phosphinate, phosphonate, phosphoramidate), and N-alkyl carboxylates, which have been extensively reviewed.[1,4] The common structural features include a moiety capable of chelating to the essential zinc metal found at the catalytic site and a peptidic fragment capable of binding to a subset of the specificity pockets of the enzymes, usually on the P' side. In the dipeptide hydroxamate class of inhibitors, the P_1' side chain (R) generally has an isobutyl group (1), although the phenylpropyl group has been used as gelatinase inhibitors.[5] The P' side hydroxamate inhibitors have potencies in the 10^{-9} molar range which would offer a stable enzyme-inhibitor complex for x-ray crystallographic studies. We have determined the crystal structures of the catalytic domains of HFC and HNC bound to a prototypical hydroxamate inhibitor (1).[6,7] A homology model for HFS was constructed from the HFC and HNC structures and had essentially identical secondary structure.[8] We have used the MMP

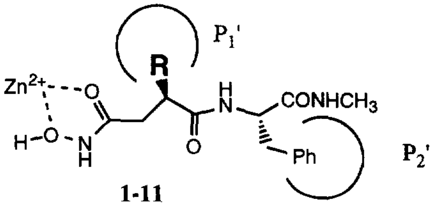

1-11

structures/model to design novel P_1' substituted hydroxamate inhibitors.

The S_1' pocket of HFC is lined at the bottom by the guanidinium functionality of Arg^{214} and contains a water molecule which is hydrogen bonded to the guanidinium group and other protein amide groups. The strategy for HFC inhibitor design was to add functionality to the P_1' group which could 1) form a salt bridge to the guanidinium group of Arg^{214}, or 2) displace the water molecule to bulk solvent by replacing the hydrogen bonding of the water molecule. The butyric acid (**4**) appeared to possess the appropriate linker to provide salt bridge formation. The alcohols (**2**, **3**, Table 1) appeared to possess the appropriate linker to displace the S_1' water molecule and replace its hydrogen bonding pattern. Also, displacement of the water molecule from the bound site to bulk water should be entropically favorable.

In the HNC structure and HFS model, residue 214 is Leu. The smaller side chain of Leu^{214} does not form the bottom of the S_1' pocket. Instead, the S_1' pocket continues in a long tunnel-like cavity. The strategy for HFS/HNC inhibitor design was to match the size of the inhibitor P_1' moiety to the size of the S_1' pocket. Since the S_1' pocket is largely hydrophobic, relatively hydrophobic benzylic (**8**, **10**) and phenolic (**9**, **11**) ethers were prepared. However, the N-H of the butyramides (**5-7**) were designed to form a hydrogen bond to the carbonyl of Tyr^{237} in the larger S_1' pocket of HNC and HFS.

The derivatives with a four-carbon atom linker were prepared from a common intermediate, **19b**, the synthesis of which is outlined in Scheme 1. The 1, 6-hexanediol (**12**) was O-alkylated with benzyl bromide (NaH, THF, reflux) to give a mixture of mono (**13**) and di-benzylated products as an approximate 2:1 mixture (60% total yield), which is subsequently used without purification. The mixture is oxidized using pyridinium dichromate (DMF, 10-25°C, 9 h) to afford a 75% yield of **14**. Oxalyl chloride converted **14** to **15**, which was subsequently used in the acylation of the chiral auxiliary, (S)-(-)-4-benzyl-2-oxazolidinone, to afford **16** in 85% yield (THF, n-BuLi, -78°C). The anion of **16**, which was formed using freshly prepared LDA, was alkylated with *t*-butyl bromoacetate to afford **17** in 55% yield. The chiral auxiliary was removed from **17** by base hydrolysis (H_2O_2, LiOH) to produce **18** in 86% yield. A coupling of **18** with L-phenylalanine N-methylamide using diethyl cyanophosphonate in DMF at 0°C yielded 85% of the common intermediate, **19b**. The above synthetic sequence has proven readily amenable to higher (5 carbon atom) and lower (3 carbon atom) homologs to afford common intermediates, **19a** and **19c**, which were further elaborated to **3**, **8**, and **11** (*vide supra*).

Scheme 2 depicts the further elaboration from **19** to the desired ether, alcohol, acid, and amide targets (**2-11**). The targeted benzylic ether (**10**) has been prepared by ester deprotection of **19b** with trifluoroacetic acid in 78% yield and conversion to the hydroxamate by reaction of the mixed anhydride of isobutyl chloroformate with O-(trimethylsilyl)hydroxylamine ($TMSONH_2$) in 59% yield. The phenolic ether (**9**) was prepared via deprotection of the benzylic ether (ammonium formate, 10% Pd/C, reflux; 64% yield) and reaction of the resultant hydroxyl intermediate (**20b**) with phenols

Scheme 1[a]

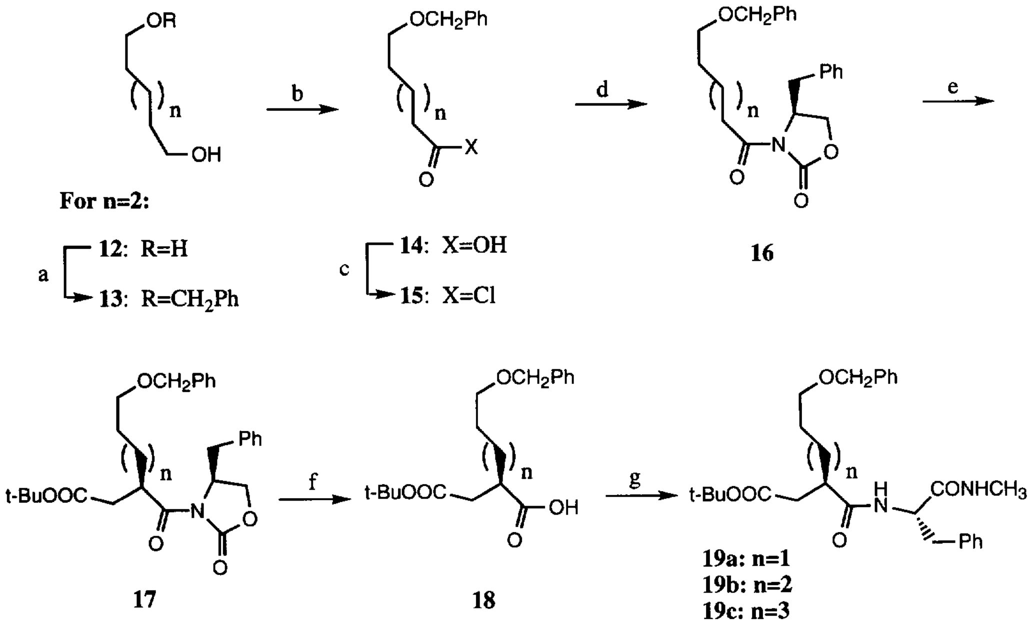

For n=2:

a: **12**: R=H → **13**: R=CH_2Ph

c: **14**: X=OH → **15**: X=Cl

16

17

18

19a: n=1
19b: n=2
19c: n=3

[a]Reagents and conditions: (a) NaH, $PhCH_2Br$, reflux, THF; (b) pyridinium dichromate, DMF, 10-25°C; (c) oxalyl chloride; (d) (S)-(-)-4-benzyl-2-oxazolidinone,THF, n-BuLi,-78°C; (e) LDA, -78°C, $BrCH_2CO_2t\text{-}Bu$; (f) H_2O_2, LiOH; (g) Diethyl cyanophosphonate, DMF, 0°C, L-phenylalanine N-methylamide.

under Mitsunobu conditions (PPh_3, Diethyl azodicarboxylate; 63% yield). The ester was deprotected and converted to the hydroxamate as described in the synthesis of **10** to give **9**. The alcohol target (**2**) was prepared from **20b** by ester deprotection and hydroxamate formation with $TMSONH_2$.

The butyric acid (**4**) was prepared from **20b** via ester deprotection and formation of a protected hydroxamate with O-(benzyl)hydroxylamine. The hydroxyl group was oxidized with pyridinium dichromate to the carboxylic acid (45% yield). Hydrogenation of the O-benzyl functionality with 10% palladium on carbon and a small amount of pyridine yielded the desired target. In a slightly different chronology, the butyramides (**5-7**) were prepared from **19b** by oxidation, conversion to the amides, and elaboration to the hydroxamate via ester deprotection and $TMSONH_2$.

An important consideration for this group of inhibitors with heteroatom moieties in the P_1' position is the larger energetic cost to desolvate these groups as they move from bulk solvent (water) into the hydrophobic environment of the S_1' pocket. If the heteroatom-based moieties, which are hydrophilic compared to hydrocarbons, do not participate in a favorable electrostatic interaction in the S_1' pocket, one expects a substantial loss in overall inhibitor potency.

Scheme 2[a]

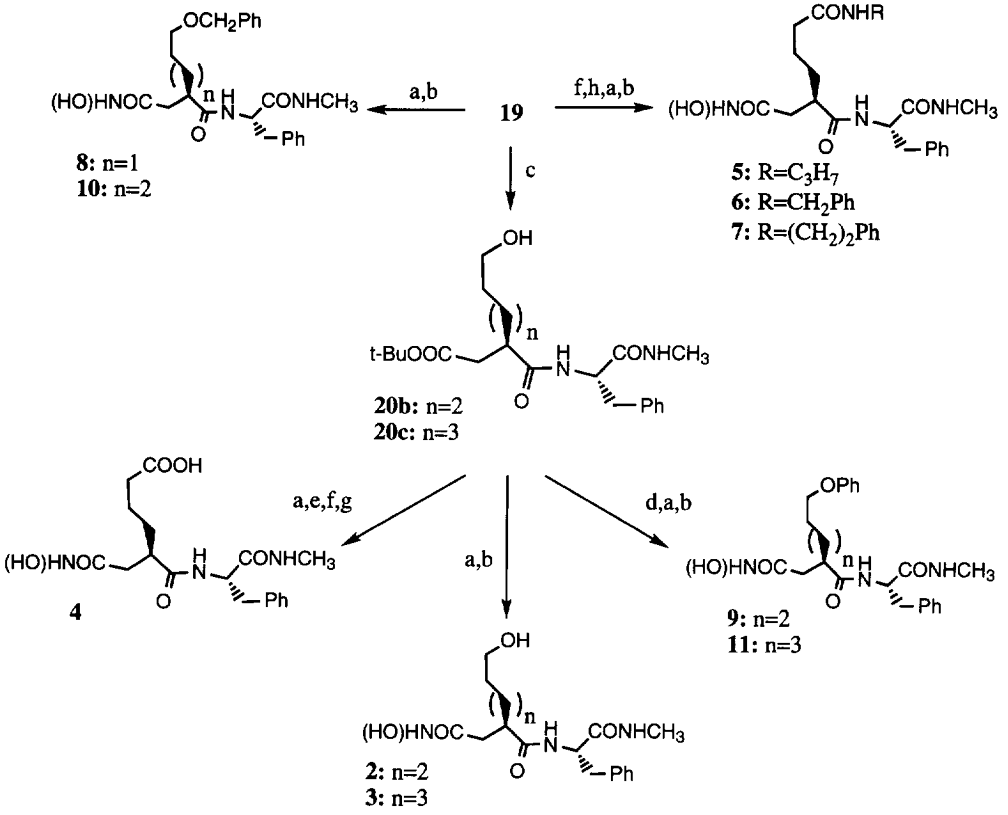

[a]Reagents and conditions: (a) TFA; (b) Isobutyl chloroformate, N-methylmorpholine, $TMSONH_2$; (c) ammonium formate, 10% Pd/C, reflux; (d) phenol, PPh_3, diethyl azodicarboxylate; (e) isobutyl chloroformate, N-methylmorpholine, $PhCH_2ONH_2$; (f) pyridinium dichromate, CH_2Cl_2; (g) H_2, 10% Pd/C, pyridine; (h) Diethyl cyanophosphonate, NH_2R.

A comparison of the data for HFC, HFS, and HNC [9] indicates that the most potent inhibition is usually found for HNC (Table 1[10]). All of the compounds (**2**-**11**) containing various linkers and overall lengths were similar in potency against HNC (10^{-8}-10^{-9} M range). The exception was **4**, which was uniformly less potent against all MMPs. The amide **5** is selective for HNC by two to three orders of magnitude in potency. Since an amide has a high desolvation cost, the potency of **5** against HNC may indicate the successful design of a specific hydrogen bond to the Tyr^{237} in the S_1' pocket of this enzyme. Proof of this awaits enzyme-inhibitor crystallographic evidence.

Table 1: Inhibitory potencies of P_1' hydroxamate derivatives

		K_i (μM)		
Compound	**R**	HFC	HFS	HNC
1	$-CH_2CH(CH_3)_2$	0.007 (0.001)	0.079 (0.017)	0.002 (0.001)
2	$-(CH_2)_4OH$	0.064 (0.004)	2.20 (0.48)	0.007 (0.003)
3	$-(CH_2)_5OH$	0.031 (0.013)	0.430 (0.22)	0.004 (0.002)
4	$-(CH_2)_3COOH$	3.35 (0.80)	>10.0	0.270 (0.060)
5	$-(CH_2)_3CONHC_3H_7$	5.10 (0.30)	0.360 (0.025)	0.002 (0.001)
6	$-(CH_2)_3CONHCH_2(Ph)$	9.6 (1.7)	0.092 (0.026)	0.030 (0.005)
7	$-(CH_2)_3CONH(CH_2)_2(Ph)$	1.3 (0.05)	0.006 (0.002)	0.032 (0.002)
8	$-(CH_2)_3OCH_2(Ph)$	2.27 (0.33)	0.043 (0.008)	<0.001
9	$-(CH_2)_4OPh$	0.008 (0.001)	0.028 (0.002)	<0.002
10	$-(CH_2)_4OCH_2(Ph)$	1.45 (0.54)	0.015 (0.004)	0.002 (0.001)
11	$-(CH_2)_5OPh$	0.026 (0.001)	0.014 (0.001)	<0.002

The HFS homology model, having an S_1' pocket essentially the same as HNC, was anticipated to have a similar inhibition profile to HNC. However, like **1**, the polar derivatives, such as alcohols, acid, and amides (**2-7**) were nearly two orders of magnitude less potent for HFS than HNC. The exceptions were the N-benzyl (**6**) and the N-phenethyl butyramide (**7**). Indeed, **7** was more potent against HFS than against HNC. The less polar, ether derivatives (**8-11**) were all potent inhibitors of HFS. It is interesting to note that all of these compounds (**6-11**), which are potent HFS inhibitors (< 100nM), contain a phenyl group at P_1'.

The targeting of HFC involved the replacement of the crystallographically observed water molecule or electrostatic interaction with the guanidinium moiety of Arg^{214}. While the potency of **1** against HFC is most likely due to hydrophobic binding and favorable desolvation, the alcohols **2** and **3** would be expected to gain potency and selectivity by displacement of the S_1' water molecule and replacement of its hydrogen bonding pattern. The decreased potency of **2** and **3** may be due to the replacement of only three of the four observed hydrogen bonding interactions of the S_1' water molecule with the guanidine and unfavorable desolvation. On the other hand, **4** was several orders of magnitude less potent than **1**. The desolvation energy cost for the carboxylic acid functionality is certainly less than the energy gain by a specific salt-bridge interaction.[11] Thus, the data would argue that salt bridge formation was not accomplished.

The obstruction of the S_1' pocket by the guanidinium moiety presumes that only small P_1' groups would be complementary to HFC. Indeed, the large benzylic ethers (**8,10**) show only μM potencies against HFC. However, surprising results were observed when the ether oxygen was transposed from the benzylic to the phenolic position. A comparison of ethers of similar overall length (**8** vs. **9**, **10** vs. **11**) indicated a unique potentcy against HFC for phenolic ethers (**9**, **11**), which would appear to be too large to occupy the crystallographically observed S_1' pocket of HFC. Molecular modelling studies suggest that it is possible that the side-chain of Arg^{214} is displaced such that a π-π interaction is formed between the electron-rich phenolic moiety and the electron-poor guanidinium moiety. Another possibility is a completely different mode of binding than that observed for **1**. The proof relies on further crystallographic studies of the enzymes with these inhibitors.

Acknowledgment: The assistance of Mr. Travis Stams and Ms. Angela Smallwood for crystallization trials and data analysis is greatly appreciated.

References and Notes

* Present address: 3-Dimensional Pharmaceuticals, Inc., 3700 Market Street, Philadelphia, PA 19104.

1. Schwartz, M. A.; VanWart, H. E. in *Progress in Medicinal Chemistry-Vol. 29*; Ellis, G. P. and Luscombe, D. K., Eds.; Elsevier Science Publishers: London,1992; Chapter 8.
2. Walakovits, L. A.; Bhardwaj, N.; Gallick, G. S.; Lark, M. W. *Arthr. Rheum.* **1992**, *35*, 35-42.
3. Woessner, E. M. *FASEB J.* **1991**, *5*, 2145-2154.
4. (a) Johnson, W. H.; Roberts, N. A.; Borkakoti, N. *J. Enzyme Inhibition* **1987**, *2*, 1-22.
   (b) Wahl, R. C.; Dunlap, R. P.; Morgan, B. A. in *Annual Reports in Medicinal Chemistry*; Bristol, J. A., Ed.; Academic Press: New York, 1990; Chapter 19, pp 177-84.
   (c) Henderson, B.; Docherty, A. J. P.; Beeley, N. R. A. *Drugs of the Future* **1990**, *15*, 495-508.
   (d) Beeley, N. R. A.; Ansell, P. J. A.; Docherty, A. J. P. *Curr. Opin. Ther. Patents* **1994**, *4*, 7-16.
5. Porter, J. R.; Millican, T. A.; Morphy, J. R.; Beeley, N. R. A. European Patent Application 489,577 A1, 1991.
6. Spurlino, J. C.; Smallwood, A. M.; Carlton, D. D.; Banks, T. M.; Vavra, K. J.; Johnson, J. S.; Cook, E. R.; Falvo, J.; Wahl, R. C.; Pulvino, T. A.; Wendoloski, J. J.; Smith, D. L. *PROTEINS: Structure, Function, and Genetics* **1994**, *19*, 98-109.
7. Stams, T.; Spurlino, J. C.; Smith, D. L.; Wahl, R. C.; Ho, T. F.; Qoronfleh, M. W.; Banks, T. M.; Rubin, B. *Nature:Structural Biology* **1994**, *1*, 119-123.
8. Mathiowetz, A. M., unpublished results.
9. Human cDNA for fibroblast collagenase and fibroblast stromelysin was obtained (Goldberg, G. I., Wilhelm, S. M., Kronberger, A., Bauer, E. A., Grant, G. A., Eisen, A. Z. *J. Biol. Chem.* **1986**, *261*, 6880-5). Human cDNA for neutrophil collagenase was obtained (Devarajan, P., Mooktiar, K., Van Wart, H. E., Berliner, N. *Blood* **1991**, *77*, 2731-2738). The MMPs are expressed in E. coli as inclusion bodies with the expression vector pET11a (Studier, F. W., Rosenberg, A. H., Dunn, J. J., Dubendorff, J. W. *Methods in Enzymology* **1990**, *185*, 60-89). Fibroblast stromelysin and neutrophil collagenase are expressed as mature enzymes with C-terminal truncations, Phe^{83}-Thr^{260} and Met^{81}-Gly^{243}, respectively. Fibroblast collagenase is expressed as a proenzyme with a C-terminal truncation, Phe^{1}-Pro^{250}. Inclusion bodies are solubilized in 6M urea, purified by ion exchange, and folded into their native conformation by removal of urea. Fibroblast collagenase is activated by incubation with aminophenylmercury. All active MMPs are purified by gel filtration. MMPs are assayed with peptide substrates based on R-Pro-Leu-Ala-Leu-X-NH-R_2, where R = H or benzoyl, X = Trp or O-methyl-Tyr, R_2 = Me or butyldimethylamino. The product is determined by fluorescence after reaction with fluorescamine with overall conditions and procedures similar to those of Fields, G. B., Van Wart, H. E., and Birkedal-Hansen, H. *J. Biol. Chem.* **1987**, *262*, 6221. The K_i values are calculated from the IC_{50} values, assuming competitive inhibition. The average of at least three deteminations is reported with the standard deviation in parentheses.
10. All compounds in Table 1 provided satisfactory elemental analysis or spectral data (^{1}H NMR, high resolution LSIMS) and were homogeneous by TLC.
11. Mitchell, J. B. O.; Thorton, J. M.; Singh, J.; Price, S. L. *J. Mol. Biol.* **1992**, *226*, 251-262.

(*Received in USA* 3 *October* 1994; *accepted* 14 *November* 1994)